HHS Public Access

Author manuscript

*J Chem Inf Model*. Author manuscript; available in PMC 2018 December 26.

Published in final edited form as:

*J Chem Inf Model*. 2017 December 26; 57(12): 3056–3069. doi:10.1021/acs.jcim.7b00536.

# Successful Identification of Cardiac Troponin Calcium Sensitizers Using a Combination of Virtual Screening and ROC Analysis of Known Troponin C Binders

**Melanie L. Aprahamian**[1], **Svetlana B. Tikunova**[2], **Morgan V. Price**[2], **Andres F. Cuesta**[2], **Jonathan P. Davis**[2], and **Steffen Lindert**[1,*]

[1]Department of Chemistry and Biochemistry, Ohio State University, Columbus, OH, 43210

[2]Davis Heart and Lung Research Institute and Department of Physiology and Cell Biology, Ohio State University, Columbus, OH, 43210

## Abstract

Calcium dependent cardiac muscle contraction is regulated by the protein complex troponin. Calcium binds to the N-terminal domain of troponin C (cNTnC) which initiates the process of contraction. Heart failure is a consequence of a disruption of this process. With the prevalence of this condition, a strong need exists to find novel compounds to increase the calcium sensitivity of cNTnC. Desirable are small chemical molecules that bind to the interface between cTnC and the cTnI switch peptide and exhibit calcium sensitizing properties by possibly stabilizing cTnC in an open conformation. To identify novel drug candidates, we employed a structure-based drug discovery protocol that incorporated the use of a relaxed complex scheme (RCS). In preparation for the virtual screening, cNTnC conformations were identified based on their ability to correctly predict known cNTnC binders using a receiver operating characteristics analysis. Following a virtual screen of the National Cancer Institute's Developmental Therapeutic Program database, a small number of molecules were experimentally tested using stopped-flow kinetics and steady-state fluorescence titrations. We identified two novel compounds, 3-(4-methoxyphenyl)-6,7-chromanediol (NSC600285) and 3-(4-methylphenyl)-7,8-chromanediol (NSC611817), that show increased calcium sensitivity of cTnC in the presence of the regulatory domain of cTnI. The effects of NSC600285 and NSC611817 on the calcium dissociation rate was stronger than that of the known calcium sensitizer bepridil. Thus, we identified a 3-phenylchromane group as a possible key pharmacophore in the sensitization of cardiac muscle contraction. Building on this finding is of interest to researchers working on development of drugs for calcium sensitization.

## Graphical abstract

*Corresponding Author: Department of Chemistry and Biochemistry, Ohio State University, 2114 Newman & Wolfrom Laboratory, 100 W. 18th Avenue, Columbus, OH 43210, 614-292-8284 (office), 614-292-1685 (fax), lindert.1@osu.edu.

This information is available free of charge via the Internet at http://pubs.acs.org

Supporting Information Available: Additional figures and detailed ROC curve results

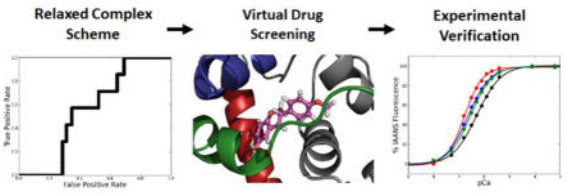


## INTRODUCTION

Heart failure, a condition that affects nearly 5.7 million Americans each year, occurs when the cardiac muscle is unable to pump enough oxygenated blood to the rest of the body resulting in improper function. Contraction of the cardiac muscle is made possible by the intricate interaction between several proteins.[1] Malfunction of any of these proteins can lead to heart failure typically due to hindered contraction. The key players in cardiac muscle contraction are the thick (made up of myosin) and the thin (containing actin, tropomyosin, and troponin) filaments.[2] Binding of myosin heads to the thin filament and subsequent conformational changes in myosin create mechanical force and ultimately contraction. This process occurs in a $Ca^{2+}$ dependent manner.[3, 4] Cardiac troponin (cTn) is a key regulatory protein nexus in this contraction process. The cardiac troponin complex consists of three subunits: troponin C (cTnC) – the subunit that binds calcium; troponin I (cTnI) – the inhibitory subunit; and troponin T (cTnT) – the subunit that secures the troponin complex to tropomyosin-actin.[4–7] The structure of all three subunits of cTn is shown in Figure 1. When $Ca^{2+}$ binds to the N-terminal regulatory domain of cardiac troponin C, cNTnC (cTnC residues 1-89), the exposure of a hydrophobic patch between the helices A and B, as shown in Figure 2, becomes more likely.[8] This pocket can bind the $cTnI_{144\text{-}163}$ switch peptide and thereby initiate contraction.[5, 9, 10]

A potential treatment for heart failure is the development of cardiac inotropes – agents that affect muscle contraction. Many different inotropes have been discovered over the years that affect the molecular landscape involved in cardiac contraction. These compounds include cardiac glycosides, β-adrenoceptor agonists, and phosphodiesterase inhibitor.[11–13] The mechanisms of these compounds all act to increase calcium levels within cardiomyocytes (*i.e.* calcium mobilizers).[14] However, adverse effects such as myocardial ischemia (decreased blood flow to the heart) and arrhythmias (abnormal heart beat)[13] directly result from the use of these inotropes. Another mechanism by which inotropes have been found to aid against heart failure is through calcium sensitization. Such calcium sensitizing compounds may affect cNTnC's calcium affinity while ideally not altering the intracellular $Ca^{2+}$ concentrations. This mechanism has the potential to avoid many of the adverse side effects associated with other drugs.[15]

The most widely studied calcium sensitizer is levosimendan.[16–18] Levosimendan is a positive inotropic compound that binds to cTnC and acts to prolong the $Ca^{2+}$ bound conformation of isolated cTnC.[17] Despite knowing the effects of levosimendan on cardiomyocytes, the exact binding mechanism on cTnC is still under debate.[16, 17, 19] Currently, no experimental structure has been obtained for levosimendan bound to cTnC, but a model has been built showing levosimendan bound to the hydrophobic pocket of cNTnC.[20]

Levosimendan has been through several clinical trials but has yet to be approved in either the US or Canada.[21] It is currently available in Europe and Japan under the trade name Simdax. Pimobendan is another positive inotrope with vasodilating effects.[22] It has undergone clinical trials and is currently used in veterinary medicine as a treatment for congestive heart failure in canines.[23–25] Another calcium sensitizing compound more recently discovered is NSC147866 which has been shown to bind to both cNTnC and the cNTnC-cTnI$_{147\text{-}163}$ complex.[10, 26] Other compounds reported to bind to the hydrophobic pocket of cNTnC are bepridil[10, 22, 27], W7[10, 28], DFBP-O[10, 26, 29], and trifluoperazine[22, 27, 30]. The chemical structures of these compounds are shown in Figure 3.

Structure-based computer aided drug discovery methods can facilitate the search for novel small molecules binding to the hydrophobic pocket of cNTnC.[31] Molecular dynamics simulations have shown that calcium-bound cNTnC exhibits significant structural flexibility, allowing it to transiently open the hydrophobic pocket between helices A and B.[8, 32, 33] Therefore methods explicitly accounting for receptor flexibility in computer-aided drug design[34] should be used for cNTnC structure-based drug discovery. The relaxed complex scheme (RCS) is a virtual screening method that accounts for both ligand and protein receptor flexibility.[35–37] Traditionally, computational docking calculations utilize static receptor structures and allow for the ligand to be flexible. The most common applications of the RCS method use multiple receptor structures obtained from a molecular dynamics (MD) simulations starting from a crystal or NMR structure that contains a docked ligand. Variations of the RCS have been successfully used in several virtual drug discovery studies[38–46], including in the identification of a low affinity calcium sensitizing agent.[26]

The RCS method used in this study was performed in conjunction with a structure-based virtual screening of a large database of compounds, a widely used screening technique.[26, 47] An alternative to a structure-based virtual screening method for identifying potential active ligands is to use a ligand-based screening method.[48, 49] This method does not depend upon knowledge of the receptor structure and relies solely upon the chemical structure and composition of the known active ligands, and machine learning techniques are then used to discover patterns in known actives. This is followed by screening large compound databases for compounds that have some degree of similarity to the active ligands. However, for cTnC the number of known active ligands is relatively small and thus excludes ligand-based screening approaches.

To identify novel compounds that demonstrate stronger calcium sensitization in cNTnC, we have employed the relaxed complex scheme to determine likely candidate compounds and experimentally verified them using a combination of stopped-flow kinetics and calcium fluorescence titrations. However, cNTnC conformations for the RCS were not selected based on purely geometric considerations (in a previous study, cNTnC conformations were picked based on an RMSD clustering analysis[26]). The goal of this study was to identify cNTnC-CTnI$_{144\text{-}163}$ conformations and a ligand preparation method that are highly predictive of $Ca^{2+}$ sensitizer binding. This was accomplished by utilizing knowledge of a set of known cNTnC binders in combination with a receiver operator characteristic analysis. Those conformations were subsequently used in RCS-type virtual screening. We experimentally tested the top compounds from the screen using stopped-flow kinetics and steady-state

fluorescence $Ca^{2+}$ titrations. This resulted in the identification of two new compounds, NSC600825 (3-(4-methoxyphenyl)-6,7-chromanediol) and NSC611817 (3-(4-methylphenyl)-7,8-chromanediol), which show promise as $Ca^{2+}$ sensitizers of cNTnC.

## METHODS AND MATERIALS

### Selection of 35 Representative cNTnC Conformations as a Test Set

A test set of cNTnC and cNTnC-$cTnI_{144-163}$ conformations was obtained from a combination of structures from the protein data bank and a 100 ns molecular dynamics (MD) simulation of DFBP-O bound cNTnC F · $Ca^{2+}$-$cTnI_{144-163}$.[26] A total of 35 different cNTnC and cNTnC-$cTnI_{144-163}$ conformations were chosen as the test set. Of the 35 conformations, five conformations were taken from crystal and NMR structures deposited in the protein data bank that had a known active compound bound to the hydrophobic pocket. Three of these conformations were cNTnC-$cTnI_{144-163}$ conformations: 1XLF [contained bepridil][50], 2KRD [contained w7][51], and 2L1R [contained DFBP-O][29]. The other two were cNTnC conformations: 1WRK [contained trifluoperazine][28] and 2KFX [contained w7][52].

The remaining thirty conformations were extracted from a 100 ns MD simulation of a calcium sensitizer (DFBP-O) bound complex of cNTnC · F $Ca^{2+}$-$cTnI_{144-163}$, the details of which have been previously reported.[26] This simulation of a DFBP-O bound complex of cNTnC F · $Ca^{2+}$-$cTnI_{144-163}$ was chosen as it corresponds to the method used to identify NSC147866. The 100 ns simulation demonstrated clear convergence after 20 ns indicating that any structures selected from the trajectory are valid representations of the conformational ensemble of the protein (see Supporting Information Figure 1). From this MD simulation, 15 frames (corresponding to snapshots of the simulation at various points in time) were chosen as potential representative conformations based upon an RMSD cluster analysis, which was detailed in the previous paper.[26] In addition, pocket-volume calculations were performed to determine additional cNTnC conformations that exhibit large hydrophobic pockets. These calculations were done using POVME.[53] Pocket volumes were calculated for each trajectory every 20 ps, resulting in 5000 pocket-volume measurements. The analysis was performed on the MD trajectory frames with the DFBP-O ligand coordinates removed. The coordinates for the inclusion sphere were extracted from coordinates of the docked ligand in the initial frame of the trajectory. A single inclusion sphere was used with a radius of 10 Å. For the conformations for the test set, 15 frames were chosen that had large pocket volumes (> 195 $Å^3$) and were distributed evenly throughout the entire 100 ns trajectory.

Prior to performing any docking calculations, each of the 35 receptor protein conformations were prepared using Schrödinger's Protein Preparation Wizard[54], resulting in conformations that were optimized and hydrogenated and therefore suitable for use with Glide XP.[55–57] The bound ligands, $Ca^{2+}$ ions, and any water molecules were removed from the conformations. The preparation process was done by first deleting all water molecules. The conformations were then repaired by filling in any missing residues. Lastly, a restrained minimization using the OPLS_2005 force field[58] was run on the protein structure with a restraint RMSD tolerance of 0.30 Å.

Finally, a receptor grid was created for each of the 35 conformations. Glide utilizes a grid-based docking algorithm that requires an active site identification.[56] This grid defines a 3D box that encompasses the coordinate space that is used for positioning the ligand. For each of the 35 receptors, a box center and dimensions were defined in this grid generation process. For receptors #1–5, the box centers were taken as the central coordinates of the experimental ligand respectively. For receptors #6–35, the center coordinates of the box corresponded to the central coordinates of the bound DFBP-O in the initial frame of the trajectory. The dimensions of the box were chosen as 15 Å in each dimension.

## Active and Decoy Ligand Test Set

A test set of 1007 ligands was compiled and contained both ligands known to be active in the hydrophobic pocket of cNTnC and ligands assumed to be inactive (referred to as decoys). A total of 7 ligands were chosen as actives. These ligands are shown in Figure 3. The known active ligand coordinates were taken from either a crystal/NMR structure (bepridil [1LXF], W7 [2KRD], DFBP-O [2L1R], trifluoperazine [1WRK]) or manually built in Maestro[59] using the known chemical structure (pimobendan, levosimendan, NSC147866). The “1K Drug-Like Ligand Decoy” set[55, 56] was chosen as the decoy set. It contained 1000 ligands with an average molecular mass of 360 Da, comparable to the average size of the known active ligands (325 Da). In terms of volume, the decoy set selected contains molecules with molecular volumes that are also comparable to the active ligand set (see Supporting Information Figure 2).

## Selection of Highly Predictive cNTnC Conformations

In addition to the protein receptor conformations used, the effect of different ligand preparation strategies on active compound enrichment was tested. To better emulate the conditions present when screening compounds in a large database which are typically provided as 2D structures (such as the NCI database), all 1007 ligands (1000 decoys and 7 actives) were converted into 2D structures prior to the preparation process. This was done in order to maintain consistency with respect to how all of the ligands were treated. LigPrep was used for the preparation of the ligands.[60] This software allows the user to add hydrogen atoms, generate various ionization states at multiple pH values using either the built-in Ionizer or Epik ionization protocols[61, 62], generate tautomers, generate alternative chiralities, and minimize the structure using a user-selected force field.[63–66] Depending upon the inputs chosen, multiple versions of each ligand could be generated (e.g. versions with different protonation states). Table 1 lists the ligand preparation strategies that were tested along with the number of generated ligands.

Subsequently, the prepared active and decoy ligands were docked using Glide XP into each of the 35 prepared receptor conformations. Each ligand was docked into each of the prepared receptor conformations. The top scoring pose of each ligand along with its docking score were extracted from the Glide XP results and used for further analysis.

A ROC (receiver operator characteristic) curve analysis was performed to measure the relative predictive ability to find hydrophobic pocket binders of each protein conformation.[67] This method of analysis is used to evaluate how well a system predicts a binary classifier

system. In this case, we were testing how well each specific protein conformation can predict the binding of known binders into the hydrophobic pocket. The ROC curves were generated by ranking the docking scores for all the active and decoy ligands for each receptor. The curve was created by plotting the number of true positives (TP) divided by the sum of true positives and false negatives (FN) versus the number of false positives (FP) divided the sum of false positives and true negatives (TN). In other words, the occurrence of the active compounds is plotted against the occurrence of the decoys in the rank-ordered list of docking scores. The axes are normalized.

A total of 105 ROC curves were generated, resulting from the 35 receptor conformations tested in combination with each of the 3 ligand preparation methods. The curves were generated using an in-house python script that reads in the output docking scores, recording only the score of the top pose for each ligand. If the ligand preparation method generated multiple versions of a ligand, only the top scoring pose out of all the possible versions is extracted, resulting in a total list of 1007 docking scores. In many cases, if a ligand scored poorly, it was not reported in the Glide XP output file. This resulted in the total number of reported docked ligands being less than the actual number of ligands used as input. To account for this, we added the ligands that do not have reported scores onto the end of the list while making the assertion that if any of those ligands were active compounds they would be placed at the very end. This was done to represent a “worst-case” scenario where the active ligands with unreported scores were assumed to dock worse than any of the unreported decoy ligands.

A combination of area under the curve (AUC) and enrichment factor was used to measure the relative predictive ability of each receptor. The AUC was calculated by rectangular integration. The enrichment factor for each receptor conformation/ligand preparation combination was calculated using:

$$EF = \frac{N_{active\ in\ top\ 40}}{40} \cdot \frac{N_{total}}{N_{actives}} = \frac{N_{active\ in\ top\ 40}}{40} \cdot \frac{1007}{7} = 3.596 \cdot N_{active\ in\ top\ 40}$$

where $N_{active\ in\ top\ 40}$ is the number of active compounds found in the top 40 (chosen based upon only being able to order a maximum of 40 compounds at a time from the NCI) scoring ligands, $N_{total}$ is the total number of docked ligands (actives + decoys, in this case a total of 1007 ligands), and $N_{actives}$ is the total number of actives (in this case 7). Although pragmatic, the decision to use a sample set of 40 for the enrichment factor provides a large enough set to demonstrate enrichment as well as ensures feasiblity for experimental follow-up. Alternative approaches have been explored for selecting the most suitable metrics, such as the null hypothesis protocol presented Hawkins and coworkers.[68] Unfortunately, due to the highly non-normal distribution of the enrichment factors, this null hypothesis method could not be applied. In theory, a perfectly random distribution of actives and decoys would result in a normalized AUC of 0.5 and an enrichment factor of 1, based upon the assumption that in a perfectly random system, the active ligands would be evenly distributed throughout the scored compound list. Normally, the results would be compared against these metrics. However, since our ligand preparation strategies generally generated multiple versions of

each ligand and only the top scoring of each ligand was used for the ROC curve, these baselines needed to be adapted for the respective ligand preparation strategies. To account for this, we developed an in-house python-based random docking score generator. The script read in the list of docked ligands for each receptor that contains the correct number of multiple versions of each and assigned each of them a random docking score ranging from 0 to 1 generated using a random number generator. AUCs and enrichment factors were calculated by extracting only the top scoring of each ligand resulting in a list of 1007 ligands. This process was repeated for thousands of iterations. The values for the AUC and the EF converged after ~50,000 iterations. Plots illustrating this convergence are shown in Supporting Information Figure 3. The calculations were repeated 50,000 times and averaged to give an AUC and enrichment factor baseline that was specific to each receptor/ligand preparation method. The baselines were determined by averaging three trials of 50,000 iterations. The raw calculated AUC and enrichment factor values for each combination along with their respective baselines can be found in Supporting Information Table 1.

Based upon the ROC curve results, three top receptor conformations were chosen along with a ligand preparation method. This was accomplished by comparing AUC and enrichment factor calculations for each receptor and ligand preparation combination to their respective baselines. A ligand preparation method was chosen first by identifying which set of 35 docking calculations had the most receptors with enrichment factors above their baselines. After selecting a ligand preparation method, three receptor conformations with the highest AUCs and enrichment factors compared to their respective baselines were chosen.

### Virtual Screen of NCI Database

The entire National Cancer Institute (NCI) open database (265,242 total compounds) was used for the virtual screen. The compounds were prepared using the ligand preparation method identified as providing the best calcium sensitizer binding predicting capability (OPLS_2005 force field for minimization, the Ionizer ionization method to generate all possible structures at a target pH of 7.4, and generating all combinations of stereoisomers with at most 5 versions generated per ligand). This ligand preparation method generated a total of 513,446 compounds. Due to the large number of compounds in the database, the virtual screening workflow was used for the screening.[67] The compounds post-LigPrep were docked into each of the three cNTnC receptor conformations selected from the test set using Glide HTVS. From these results, the top 10% for each receptor (26,000 compounds for each of the three receptors; after ligand preparation: 54,685 for #16, 49,604 for #19, and 49,017 for #28) were then docked into the three receptors using Glide SP. Finally, the top 10% of the SP results for each receptor (2,600 compounds for each of the three receptors; after ligand preparation: 6,319 for #16, 5,292 for #19, and 5,734 for #28) were docked into all three receptors using Glide XP.

Using a custom python script, the results from the Glide XP docking for each receptor were analyzed. The script reported all compounds that appeared in the top 100 scoring for all three receptors, in addition to the top 15 scoring ligand poses for each receptor individually and the compounds in ranked order averaged across all three receptors. From these results, a set of compounds was chosen for experimental testing. One of the compounds appeared in

the top 100 scoring for all three receptors and the remaining compounds were chosen from the ranked list of averaged scores with preference being given to compounds that occurred in the top 15 of any of the three receptors.

In addition, a subset of the NCI database was also screened. This subset contained all the compounds from the database that are structurally similar to NSC147866 (Tanimoto index > 80%), a previously determined calcium sensitizing agent found in the NCI database.[26] This subset contained a total of 336 compounds. Using the same method for ligand preparation, the ligands were docked into each of the top three receptors using Glide XP. The same script used for the entire database analysis was used. A check was added to ensure that there were no duplicates with the set determined from the entire database. Another set of compounds were selected from this list. These compounds were ordered from the NCI Developmental Therapeutics Program (DTP) for potential experimental verification.

Based upon the experimental screening of a portion of the compounds using stopped flow, NSC600285 was identified as a potential $Ca^{2+}$ sensitizer. A final screen was then performed on compounds structurally similar to NSC600285 (Tanimoto index > 80%). The subset contained 68 different compounds. The same procedure was followed as was used for NSC147866.

## Proteins and Ligands Utilized for Experimental Verification

The pET3a plasmid encoding human cardiac troponin C (cTnC) was a generous gift from Dr. Lawrence B. Smillie (University of Alberta, Edmonton, AB). The $cTnC^{C35S}$ mutant was generated, expressed, purified and labeled with environmentally sensitive fluorescent probe IAANS on $Cys^{84}$ as previously described.[69] The $cTnI_{128\text{-}180}$ peptide was synthesized by The Ohio Peptide, LLC (Powell, OH). The cTnC-cTnI chimera (utilized for initial compound screening) was generated, expressed, purified and labeled with IAANS on $Cys^{53}$ as previously described.[70]

The ligands were obtained from the National Cancer Institute Developmental Therapeutics Program. The samples obtained ranged between 5 and 10 mg. Bepridil was purchased from Sigma-Aldrich. The samples were dissolved in DMSO to a stock concentration of 50 mM.

## Steady-State Fluorescence Measurements

All steady-state fluorescent measurements were carried out using Perkin-Elmer LS55 fluorescence spectrometer at 15°C. IAANS fluorescence was excited at 330 nm and monitored at 450 nm as μL amounts of $CaCl_2$ were added to 2 mL of IAANS-labeled $cTnC^{C35}$ (0.25 μM) in the presence of $cTnI_{128\text{-}180}$ peptide (1.25 μM), in the absence or presence of compound (100 μM), in titration buffer (200 mM MOPS (to prevent pH chances upon addition of $Ca^{2+}$), 150 mM KCl, 2 mM EGTA, at pH 7.0), with constant stirring. The $[Ca^{2+}]_{free}$ was calculated using the computer program EGCA02 developed by Robertson and Potter.[71] The $Ca^{2+}$ sensitivities were reported as a dissociation constant $K_d$, representing a mean of at least three separate titrations ± SE. The data were fit with a logistic sigmoid function (mathematically equivalent to the Hill equation). As a control against potential aggregation, the above measurements were repeated in the presence of 0.025% zwitterionic detergent Tween-80.

### Stopped-Flow Fluorescence Measurements

All kinetic measurements were carried out using an Applied Photophysics Ltd. (Leatherhead, UK) model SX.18MV stopped-flow apparatus with a dead time of ~1.4 ms. IAANS fluorescence was excited at 330 nm with emission monitored through a 420–470 nm band-pass interference filter (Oriel, Stratford, CT). EGTA (10 mM) in stopped-flow buffer (10 mM MOPS, 150 mM KCl, at pH 7.0) was utilized to remove $Ca^{2+}$ (500 μM) from IAANS labeled $cTnC^{C35S}$ (0.5 μM) in the presence of $cTnI_{128-180}$ peptide (2.5 μM in the stopped-flow buffer at 15°C. 100 μM of each compound were individually added to both stopped-flow reactants to screen the compounds. The data were fit using a program (by P.J. King, Applied Photophysics Ltd. that utilizes the nonlinear Levenberg-Marquardt algorithm. Each $k_{off}$ represents an average of at least three separate experiments ± SE, each averaging at least five shots fit with a single exponential equation.

### Statistics

Experimental results obtained from the steady-state $Ca^{2+}$ binding as well as the $Ca^{2+}$ dissociation rates, were compared by a one-way ANOVA followed by a Tukey's HSD (honest significant difference) post-hoc test. A value of $p < 0.05$ was statistically significant.

## RESULTS AND DISCUSSION

Previous studies using computer-aided drug discovery targeting cTnC have used either experimental cTnC structures (from X-ray crystallography or NMR) or geometrically representative snapshots from molecular dynamics simulations as receptors.[26] However, the cNTnC conformations used in the virtual screens were never selected based upon their ability to correctly predict known cNTnC binders. In this study, prior to performing any type of virtual drug screening, we ensured that the static protein conformations to be used as receptors were predictive of binding calcium sensitizing compounds. The test set of cNTnC and cNTnC-cTnI144-163 conformations, totaling 35 structures, were chosen from a combination of experimental crystal/NMR structures obtained from the protein databank and frames extracted from a molecular dynamics trajectory of an NMR complex of DFBP-O bound cNTnC · F Ca2+-cTnI144-163 (PDB 2L1R). Figure 4 summarizes our drug discovery protocol.

### Generation of an Ensemble of cNTnC Conformations that Represent the Structural Flexibility of the Hydrophobic Patch

A pre-selection of cNTnC and cNTnC-$cTnI_{144-163}$ conformations that represent the structural ensemble of cardiac TnC in solution was made to subsequently identify which of those conformations is most predictive for drug discovery. A total of five crystal/NMR structures were selected, all of which contain an active compound bound to either cNTnC or cNTnC-$cTnI_{144-163}$. Three of these conformations have actives bound to cNTnC-$cTnI_{144-163}$: 1XLF [contains bepridil][50], 2KRD [contains w7][51], and 2L1R [contains DFBP-O][29]. The other conformations contain active ligands that are bound to just cNTnC: 1WRK [contains trifluoperazine][28] and 2KFX [contains w7][52]. The coordinates for the docking location were chosen as the central coordinates of the docked ligand in each respective structure. These conformations account for receptors #1–5.

The remaining thirty structures were extracted from a MD simulation of DFBP-O bound cNTnC · F $Ca^{2+}$-$cTnI_{144-163}$ (PDB 2L1R). Using POVME, the pocket volume for each frame corresponding to every 20 ps of the 100 ns trajectory was calculated. The volumes plotted as a function of time are shown in Figure 5. Fifteen frames were chosen that have volumes ranging from 106 - 258 $Å^3$ and were dispersed evenly throughout the trajectory. The selection of larger pockets in the MD simulation was based on reports that screening of larger pocket conformations has been associated with improved outcomes in drug discovery.[72, 73] The volumes and relative RMSDs of each of these 15 conformations are shown in Table 2. These defined structures #6–20. The final fifteen structures, #21–35, were extracted from the MD trajectory using a cluster analysis. The details of the RMSD cluster analysis can be found in a previous paper.[26] The docking site location for receptors #6–35 was chosen as the central coordinates of the bound DFBP-O in the initial frame of the MD simulation.

The 35 receptor conformations selected for the test set are structurally similar, but have varying properties making them all excellent candidates. The RMSDs (calculated to the experimental structure 2L1R) range from 3.08 Å to 5.88 Å over residues 1–89 and from 2.32 Å to 3.70 Å over just helices A and B. Because all of the receptor conformations initially contained a bound ligand, helices A and B are in an open conformation thus creating a sizable hydrophobic pocket. This is necessary for further virtual drug screening as there needs to be enough volume in the pocket to accommodate ligands of variable sizes.

## Selection of a Ligand Preparation Method and Three cNTnC Conformations that most Accurately Predict Binding of Known cNTnC Binders

Following the assembly of an ensemble of 35 representative cNTnC and cNTnC-$cTnI_{144-163}$ conformations, we used knowledge about known cTnC binders to identify three out of the 35 cNTnC conformations that have the highest predictive value for cNTnC binding. We docked known cNTnC binders and decoy ligands into all 35 cNTnC conformations and then selected the three conformations that ranked known ligands best with respect to decoys (see Figure 6).

In addition to the protein receptor conformations used, it was important to use a ligand preparation method that gives ligand structures that are highly predictive of binding to the hydrophobic pocket in cNTnC. Several of the ligand databases that are commonly used for virtual drug screening often only provide ligands as 2D structures that generally do not encode the correct ionization state or chirality. Using LigPrep[60], three different ligand preparation methods were tested on the 7 active ligands and 1000 decoy ligands. A list of the methods tested is shown in Table 1. The total ligand test set (1007 total ligands) was docked into each of the 35 cNTnC and cNTnC-$cTnI_{144-163}$ conformations in the test set and the docked ligands were ranked by their docking score.

For each ligand preparation method and cNTnC conformation, a ROC curve was generated that assesses how well known active ligands can be ranked in relation to inactive decoys for that particular ligand preparation method and receptor cNTnC conformation (see Supporting Information Figure 4). This allowed identification of particular cNTnC conformations that are most predictive of finding known cNTnC binders, i.e. conformations that rank the active

compounds higher compared to the decoys. The area under the ROC curve (AUC) and an enrichment factor were calculated for each receptor conformation/ligand preparation method pair and compared to a baseline specific to each system. Typically, a ROC curve has an AUC baseline of 0.5 and enrichment factor of 1 (both of which demonstrate the system being evenly distributed). In this case, each system's baseline value had to be adjusted since the ligand preparation methods used generated multiple versions of the same ligand (various ionization states for example). This was accomplished by averaging the AUC and enrichment factors over 50,000 test runs using random docking scores. The results from these calculations are shown in Table 3. AUCs and enrichment factors above the respective baseline values are an indication of how well a particular system (composed of both the receptor conformation and ligand preparation method) can predict true active ligand binding to the hydrophobic pocket of cNTnC. These two metrics were used to determine the optimal ligand preparation method along with three representative cNTnC conformations.

The ligand preparation method found to have the most receptors with enrichment factors above their respective baselines was LigPrep Method 3 (see Table 3). This method used the OPLS_2005 force field for minimization, the Ionizer ionization method to generate all possible structures at a target pH of 7.4, and generated all combinations of stereoisomers with at most 5 versions generated per ligand. This ligand preparation method was chosen as the method to be used for the prospective virtual screening to identify novel calcium sensitizing agents.

Within LigPrep Method 3, each of the individual receptors' ROC curves were analyzed. The three receptors chosen as most predictive of active binding (receptors #16, 19, and 28) were selected based upon how far their respective AUCs and enrichment factors were above the respective baselines. The relative AUC values for each of these three receptors are 0.12, 0.08, and 0.04. Most critical in the selection of these particular receptor conformations were the enrichment factors. The respective enrichment factors for each receptor were 2.42, 2.56, and 9.55. Receptor #28 exhibited the largest enrichment factor indicating that it had ranked the most active compounds within the top 40 docked ligands. These other two receptors also had elevated enrichment factors when compared to their respective baselines. Receptors #16 and 19 were extracted from the pocket-volume analysis, while receptor #28 originated from the RMSD cluster analysis of the MD simulation of DFBP-O bound cNTnC F · $Ca^{2+}$-$cTnI_{144\text{-}163}$ (PDB 2L1R). The three receptors chosen for the virtual screen are shown in Figure 6. The pairwise RMSDs for the three receptor conformations were 3.173 Å, 3.274 Å, and 3.498 Å, respectively. The pocket volumes for the three receptors, as calculated with POVME, were 171 $Å^3$, 106 $Å^3$, and 108 $Å^3$, respectively. These volumes fall within the range of volumes for the receptor conformations in the test set extracted from the MD trajectory. The lack of distinguishing features amongst the three chosen receptor conformations demonstrates the value of the ROC analysis. Without said analysis, there was no obvious reason to select the conformations that were selected. All three receptors selected originated from the MD simulation with DFBP-O bound and were complexed with the switch peptide, $cTnI_{144\text{-}163}$. The lack of experimental structures in this final set of the three most predictive cNTnC conformations underscores the importance of using MD in accounting for receptor flexibility in virtual screening. Encouragingly, in both receptors #19

and 28, DFBP-O appeared in the list of top 40 docking score compounds. This is indicative of these conformations having a high predictive value for predicting active docking.

## Virtual Screen to Identify Novel Calcium Sensitizing Agents

After identification of a predictive ligand preparation method and three predictive cNTnC conformations, we performed virtual screening of the entire NCI database using Schrödinger's virtual screening workflow to identify novel compounds that are potential $Ca^{2+}$ sensitizers for cNTnC. We hypothesized that using this particular combination of three receptor conformations and ligand preparation method in the virtual screen would increase the chances of identifying active calcium sensitizing molecules that bind to the hydrophobic pocket. The receptor conformations and ligand preparation method used for the compounds in the database were identified as being highly predictive of binding to the hydrophobic pocket.

The virtual screen was performed by docking all compounds first using Glide HTVS, then docking the top 10% for each receptor using Glide SP, and then finally docking the top 10% of those using Glide XP. After the virtual screening, a set of the top scoring compounds were chosen. These compounds were based on analyzing the average docking score across all three receptor conformations as well as identifying compounds that occurred in the top 100 scoring for all three receptor conformations. The selection was based on compounds having good scores in all three receptor conformations. Only a single compound (NSC254212) was found in the top 100 of all three receptor conformations and coincidentally had the best average docking score. The remaining compounds were chosen from the ranked list of averaged scores with preference being given to compounds that occurred in the top 15 of any of the three receptors. A second screen was performed on compounds within the NCI database that were structurally similar to NSC147866, a compound that we recently identified to be a weakly binding calcium sensitizer. We hypothesized that a derivative of NSC147866 might have a high probability of binding to the hydrophobic pocket. The compounds chosen were also filtered based upon availability for ordering from the NCI DTP. Only compounds that were available for ordering were chosen. The compounds selected along with their molecular weights and average docking scores (across all 3 receptors) are shown in Table 4.

A final screen was performed on compounds from the NCI database that were structurally similar to NSC600285, a compound that was identified from the initial set of compounds to bind cNTnC and show calcium sensitizing properties (see the Experimental Verification section for details). Based upon this screen, additional compounds were selected using the same selection methodology used for the other screens.

Samples of the compounds (5–10 mg of each) identified through the virtual screening process were ordered from the NCI DTP. The compounds were screened using stopped-flow and the two promising candidates were subsequently tested for their ability to act as calcium sensitizers. Partly because of solubility issues and inner filter effects, only a portion of the compounds were successfully screened.

## Experimental Verification

The two potential $Ca^{2+}$ sensitizers (NSC600285 and NSC611817) were initially identified via stopped-flow screening using the cTnC-cTnI chimera.[70] Since changes in $Ca^{2+}$ sensitivity can be caused by either changes in $Ca^{2+}$ dissociation or association rate, or a combination of both rates we needed to determine whether the two compounds were in fact $Ca^{2+}$ sensitizers. The effects of the compounds on $Ca^{2+}$ sensitivity of cTnC in the presence of $cTnI_{128\text{-}180}$ were measured by following the $Ca^{2+}$ induced changes in fluorescence of IAANS-labeled $cTnC^{C35S}$ using steady-state fluorescence titrations. We determined that both compounds led to an increase in calcium sensitivity of IAANS-labeled $cTnC^{C35S}$ in the presence of $cTnI_{128\text{-}180}$ (Figure 7A). The increase in $Ca^{2+}$ sensitivity is apparent by the left shift (decrease in $K_d$) of the steady-state curves. A one-way ANOVA followed by a Tukey's HSD analysis indicated that both compounds show a statistically significant increase in calcium sensitivity when compared to the control.

We also compared the $Ca^{2+}$ sensitizing effects of the two new compounds to that of a known $Ca^{2+}$ sensitizer, bepridil.[74] The $Ca^{2+}$ induced increases in IAANS fluorescence, which occur when $Ca^{2+}$ binds to the regulatory N-domain of IAANS-labeled $cTnC^{C35S}$ in the presence of $cTnI_{128\text{-}180}$, in the absence or presence of NSC600285, NSC611817, or bepridil are shown in Figure 7A. In the presence of $cTnI_{128\text{-}180}$, the IAANS-labeled $cTnC^{C35S}$ exhibited a half-maximal $Ca^{2+}$-dependent increase in IAANS fluorescence at 0.60 ± 0.03 μM. NSC600285, NSC611817 and bepridil led to ~2.4-, 2.1- and 2.0-fold increases, respectively, in the $Ca^{2+}$ sensitivity of the IAANS-labeled $cTnC^{C35S}$ in the presence of $cTnI_{128\text{-}180}$. Statistical analysis using a combination of one-way ANOVA and Tukey's HSD test indicated that the $Ca^{2+}$ sensitizing effects of the two new compounds was similar to that of the known compound, bepridil. The Hill Coefficients (steepness) for all the curves fell within 1.03 to 1.13 indicating a non-cooperative binding event.[75]

To confirm the initial stopped-flow screening results, further stopped-flow experiments were conducted to determine the effect of the two identified compounds on the kinetics of $Ca^{2+}$ dissociation from cTnC in the presence of $cTnI_{128\text{-}180}$. Effects were also compared to that of bepridil. Figure 7B shows that excess EGTA removed $Ca^{2+}$ from the regulatory N-domain site of IAANS-labeled $cTnC^{C35S}$, in the presence of $cTnI_{128\text{-}180}$, at ~106 ± 2 $s^{-1}$. NSC600285, NSC611817 and bepridil led to ~2.5-, 2.3- and 1.7-fold deceleration in the rate of $Ca^{2+}$ dissociation from IAANS-labeled $cTnC^{C35S}$ in the presence of $cTnI_{128\text{-}180}$. Statistical analysis using one-way ANOVA and Tukey's HSD test showed that all three compounds significantly slowed the rate of $Ca^{2+}$ dissociation from IAANS-labeled $cTnC^{C35S}$ in the presence of $cTnI_{128\text{-}180}$. Furthermore, the two new compounds led to a significantly slower $Ca^{2+}$ dissociation from IAANS-labeled $cTnC^{C35S}$ compared to that of bepridil. Our results indicate that the $Ca^{2+}$ sensitization caused by all three compounds was largely due to deceleration in the $Ca^{2+}$ dissociation rate.

The two compounds were filtered against the PAINS moieties (Pan Assay Interference Compounds) to ensure that both compounds were true positives[76]. PAINS compounds are compound moieties that are frequent hits in high throughput drug screens and have properties that lead to apparent activity in multiple assays[77]. NSC600285 and NSC611817 were analyzed using the FAFDrugs4 program utilizing filters for all three classes of PAINS

compounds[78–80]. Both compounds were identified as intermediate molecules due to the catechol functional group[81, 82]. Compounds with this functional group can potentially aggregate and provide indeterminate experimental results.

In order to show that NSC600285 and NSC611817 are displaying true activity and are not aggregating, we repeated the $Ca^{2+}$ titrations in the presence of the zwitterionic detergent Tween-80 (0.025%) as recommended to rule out potential PAINS effects.[83] In the presence of Tween-80, both compounds still statistically $Ca^{2+}$ sensitized $cTnC^{C35S}$ in the presence of $cTnI_{128\text{-}180}$ (Figure 7C). Additionally, we measured the effect of the compound NSC603663 which did not pass our initial screening, since it did not affect the rate of $Ca^{2+}$ dissociation from the cTnC-cTnI chimera. Compound NSC603663 was selected because it also contains a catechol group. Figure 7D demonstrates that NSC603663 did not $Ca^{2+}$ sensitize $cTnC^{C35S}$ in the presence of $cTnI_{128\text{-}180.}$ Thus, the presence of catechol group by itself is not sufficient to affect our assay.

In addition to potential aggregation, the catechol groups in the compounds pose the potential to oxidize and form ortho-quinones. Docking calculations were performed on the oxidized forms of NSC600285 and NSC611817. The docking scores averaged over all three receptors for the unoxidized (catechol) forms of NSC600285 and NSC611817 were −7.69 and −10.21 respectively. The oxidized (ortho-quinone) forms gave significantly worse docking scores of −4.90 and −6.23, respectively, strongly suggesting that the unoxidized group is the dominant bound form. Should these compounds be developed further, additional experiments need to be performed to verify the binding of the unoxidized and oxidized forms and this will be explored in future work.

The two compounds identified, NSC600285 and NSC611817, belong to a class of isoflavans and have been previously discovered as being potential inhibitors for human lipoxygenases (hLO).[84] Both compounds were identified as demonstrating high selectivity and potency for 15-hLO-1 (reticulocyte 15-human lipoxygenase-1, which has been implicated in atherogenic processes) [85, 86] and inhibition of 12-hLO (platelet 12-human lipoxygenase). Thus, in addition to the $Ca^{2+}$ sensitization, these compounds could also be beneficial for the treatment of heart failure via inhibition of 15-hLO-1 and 12-hLO.[87]

## CONCLUSION

In this study, the relaxed complex scheme (RCS) was employed to identify novel compounds that increase calcium sensitization of cNTnC. In contrast to previous studies, in preparation for the virtual screening, cNTnC conformations were identified based on their ability to correctly predict known cNTnC binders. The large NCI DTP database was subsequently screened against those particular cNTnC conformations and 40 compounds were ordered for testing. A portion of the compounds identified in the virtual screen (30 total) were tested using stopped-flow kinetics and two of the compounds that were found to show $Ca^{2+}$ sensitizing properties were then tested using steady-state fluorescence titrations. Using this methodology, we have successfully identified two novel compounds, NSC600285 and NSC611817, both of which showed increased calcium sensitization (~2.4 fold) and a slowed calcium dissociation rate (~2.5 fold). These effects on the rate of $Ca^{2+}$ dissociation are

stronger than for bepridil, a known calcium sensitizer. Titration experiments in the presence of detergent Tween-80 ruled out the possibility of false positive assay results due to aggregation caused by the catechol functional groups. The chemical structures of NSC600285 (3-(4-methoxyphenyl)-6,7-chromanediol) and NSC611817 (3-(4-methylphenyl)-7,8-chromanediol) are shown in Figure 8. We speculate that the 3-phenylchromane scaffold, which contains the pharmacophore chromane (a heterocyclic compound also known as benzodihydropan), is crucial in cNTnC binding and calcium sensitization. These compounds had average docking scores into the three receptor conformations chosen through the RCS of −7.69 and −10.21 respectively. For both compounds, the docking results show that there is a T-shaped π-π interaction between the chromane portion and Phe 77 in cNTnC. NSC600285 also shows hydrogen bonding with the backbone of Ala 95. The docked poses of these compounds along with Phe 77 are depicted in Figure 9. NSC600285 was selected from the screen of the entire database and NSC611817 was selected from the subsequent screen of compounds structurally similar to NSC600285. Both compounds have low Tanimoto similarity coefficients when compared to the 7 known active compounds. The maximum common substructure Tanimoto similarity coefficients, as calculated using ChemMine Tools[88], ranged from 17% to 39% for NSC600285 and 18% to 36% for NSC611817. This suggests that the relaxed complex scheme in combination with the identification of conformations that are predictive of binding was successful in identifying truly novel compounds. We would have never screened NSC600285 and NSC611817 based on their similarity to other known active compounds. Finally, despite the successful identification of a novel pharmacophore and two calcium sensitizers, solubility proved to be a limiting factor in the experimental verification (several of the compounds screened experimentally could not be tested due to severe solubility issues). It is not surprising that the virtual screen proposes hydrophobic compounds to bind to the hydrophobic pocket of troponin C. However, this suggests that successful compounds need to exhibit a delicate balance between hydrophobic and hydrophilic groups. Future work will focus on including predicted solubility into the virtual screen to dramatically increase the number of compounds that can be tested experimentally.

In conclusion, we have identified two novel $Ca^{2+}$ sensitizers, NSC600285 and NSC611817. The $Ca^{2+}$ sensitization effects of the two compounds were largely due to slower rate of $Ca^{2+}$ dissociation. Thus, the use of our relaxed complex scheme and virtual screening in combination with experimental verification shows great promise in discovering new compounds that could one day be used to treat heart disease.

## Supplementary Material

Refer to Web version on PubMed Central for supplementary material.

## Acknowledgments

**Funding Sources**

Research reported in this publication was supported in part by the NIA institute of NIH under Award Number R03 AG054904 (to SL) and the NHLBI institute of NIH under Award Number R01 HL132213 (to JPD) and R01 HL138579 (to JPD). The content is solely the responsibility of the authors, and does not necessarily represent the official views of the NIH.

The authors would like to thank the members of the Lindert group for useful discussions and Dr. Jalal Siddiqui for the generation of the cTnC-cTnI chimera used in the initial experimental screening. We would like to thank the Ohio Supercomputer Center for valuable computational resources.[90]

## References

1. Biesiadecki BJ, Davis JP, Ziolo MT, Janssen PML. Tri-modal regulation of cardiac muscle relaxation; intracellular calcium decline, thin filament deactivation, and cross-bridge cycling kinetics. Biophysical Reviews. 2014; 6:273–289.
2. Katrukha IA. Human cardiac troponin complex. Structure and functions. Biochemistry (Moscow). 2013; 78:1447–1465. [PubMed: 24490734]
3. Marks AR. Calcium and the heart: a question of life and death. The Journal of Clinical Investigation. 2003; 111:597–600. [PubMed: 12618512]
4. Gordon AM, Homsher E, Regnier M. Regulation of contraction in striated muscle. Physiol Rev. 2000; 80:853–924. [PubMed: 10747208]
5. Kobayashi T, Jin L, Tombe PPd. Cardiac thin filament regulation. Pflügers Archiv - European Journal of Physiology. 2008; 457:37–46. [PubMed: 18421471]
6. Filatov VL, Katrukha AG, Bulargina TV, Gusev NB. Troponin: structure, properties, and mechanism of functioning. Biochemistry Biokhimiia. 1999; 64:969–985. [PubMed: 10521712]
7. Tikunova SB, Davis JP. Designing Calcium-sensitizing Mutations in the Regulatory Domain of Cardiac Troponin C. Journal of Biological Chemistry. 2004; 279:35341–35352. [PubMed: 15205455]
8. Lindert S, Kekenes-Huskey Peter M, McCammon JA. Long-Timescale Molecular Dynamics Simulations Elucidate the Dynamics and Kinetics of Exposure of the Hydrophobic Patch in Troponin C. Biophysical Journal. 2012; 103:1784–1789. [PubMed: 23083722]
9. Williams MR, Lehman SJ, Tardiff JC, Schwartz SD. Atomic resolution probe for allostery in the regulatory thin filament. Proceedings of the National Academy of Sciences. 2016; 113:3257–3262.
10. Li MX, Hwang PM. Structure and function of cardiac troponin C (TNNC1): Implications for heart failure, cardiomyopathies, and troponin modulating drugs. Gene. 2015; 571:153–166. [PubMed: 26232335]
11. Scholz H. Inotropic drugs and their mechanisms of action. Journal of the American College of Cardiology. 1984; 4:389–397. [PubMed: 6330195]
12. Francis GS, Bartos JA, Adatya S. Inotropes. Journal of the American College of Cardiology. 2014; 63:2069–2078. [PubMed: 24530672]
13. Hasenfuss G, Teerlink JR. Cardiac inotropes: current agents and future directions. European Heart Journal. 2011; 32:1838–1845. [PubMed: 21388993]
14. Pollesello P, Papp Z, Papp JG. Calcium sensitizers: What have we learned over the last 25years? International Journal of Cardiology. 2016; 203:543–548. [PubMed: 26580334]
15. Shettigar V, Zhang B, Little SC, Salhi HE, Hansen BJ, Li N, Zhang J, Roof SR, Ho H-T, Brunello L, Lerch JK, Weisleder N, Fedorov VV, Accornero F, Rafael-Fortney JA, Gyorke S, Janssen PML, Biesiadecki BJ, Ziolo MT, Davis JP. Rationally engineered Troponin C modulates in vivo cardiac function and performance in health and disease. Nature Communications. 2016; 7:10794.
16. Papp Z, Édes I, Fruhwald S, De Hert SG, Salmenperä M, Leppikangas H, Mebazaa A, Landoni G, Grossini E, Caimmi P, Morelli A, Guarracino F, Schwinger RHG, Meyer S, Algotsson L, Wikström BG, Jörgensen K, Filippatos G, Parissis JT, González MJG, Parkhomenko A, Yilmaz MB, Kivikko M, Pollesello P, Follath F. Levosimendan: Molecular mechanisms and clinical implications: Consensus of experts on the mechanisms of action of levosimendan. International Journal of Cardiology. 2012; 159:82–87. [PubMed: 21784540]
17. Haikala H, Kaivola J, Nissinen E, Wall Pi, Levijoki J, Lindén I-B. Cardiac troponin C as a target protein for a novel calcium sensitizing drug levosimendan. Journal of Molecular and Cellular Cardiology. 1995; 27:1859–1866. [PubMed: 8523447]
18. Hasenfuss G, Pieske B, Castell M, Kretschmann B, Maier LS, Just H. Influence of the Novel Inotropic Agent Levosimendan on Isometric Tension and Calcium Cycling in Failing Human Myocardium. Circulation. 1998; 98:2141–2147. [PubMed: 9815868]

19. Sorsa T, Heikkinen S, Abbott MB, Abusamhadneh E, Laakso T, Tilgmann C, Serimaa R, Annila A, Rosevear PR, Drakenberg T, Pollesello P, Kilpeläinen I. Binding of Levosimendan, a Calcium Sensitizer, to Cardiac Troponin C. Journal of Biological Chemistry. 2001; 276:9337–9343. [PubMed: 11113122]
20. Pollesello P, Ovaska M, Kaivola J, Tilgmann C, Lundström K, Kalkkinen N, Ulmanen I, Nissinen E, Taskinen J. Binding of a new Ca2+ sensitizer, levosimendan, to recombinant human cardiac troponin C. A molecular modelling, fluorescence probe, and proton nuclear magnetic resonance study. Journal of Biological Chemistry. 1994; 269:28584–28590. [PubMed: 7961805]
21. Nieminen MS, Fruhwald S, Heunks LMA, Suominen PK, Gordon AC, Kivikko M, Pollesello P. Levosimendan: current data, clinical use and future development. Heart, Lung and Vessels. 2013; 5:227–245.
22. Ovaska M, Taskinen J. A model for human cardiac troponin C and for modulation of its Ca2+ affinity by drugs. Proteins: Structure, Function, and Bioinformatics. 1991; 11:79–94.
23. Walter M, Liebens I, Goethals H, Renard M, Dresse A, Bernard R. Pimobendane (UD-CG 115 BS) in the treatment of severe congestive heart failure. An acute haemodynamic cross-over and double-blind study with two different doses. British Journal of Clinical Pharmacology. 1988; 25:323–329. [PubMed: 3282531]
24. Boyle KL, Leech E. A review of the pharmacology and clinical uses of pimobendan. Journal of Veterinary Emergency and Critical Care. 2012; 22:398–408. [PubMed: 22928748]
25. Fitton A, Brogden RN. Pimobendan. A review of its pharmacology and therapeutic potential in congestive heart failure. Drugs & Aging. 1994; 4:417–441. [PubMed: 8043944]
26. Lindert S, Li MX, Sykes BD, McCammon JA. Computer-Aided Drug Discovery Approach Finds Calcium Sensitizer of Cardiac Troponin. Chemical Biology & Drug Design. 2015; 85:99–106. [PubMed: 24954187]
27. Kleerekoper Q, Liu W, Choi D, Putkey JA. Identification of Binding Sites for Bepridil and Trifluoperazine on Cardiac Troponin C. Journal of Biological Chemistry. 1998; 273:8153–8160. [PubMed: 9525919]
28. Oleszczuk M, Robertson IM, Li MX, Sykes BD. Solution structure of the regulatory domain of human cardiac troponin C in complex with the switch region of cardiac troponin I and W7: The basis of W7 as an inhibitor of cardiac muscle contraction. Journal of Molecular and Cellular Cardiology. 2010; 48:925–933. [PubMed: 20116385]
29. Robertson IM, Sun Y-B, Li MX, Sykes BD. A structural and functional perspective into the mechanism of Ca2+-sensitizers that target the cardiac troponin complex. Journal of Molecular and Cellular Cardiology. 2010; 49:1031–1041. [PubMed: 20801130]
30. Feldkamp MD, O'Donnell SE, Yu L, Shea MA. Allosteric effects of the antipsychotic drug trifluoperazine on the energetics of calcium binding by calmodulin. Proteins: Structure, Function, and Bioinformatics. 2010; 78:2265–2282.
31. Leelananda SP, Lindert S. Computational methods in drug discovery. Beilstein Journal of Organic Chemistry. 2016; 12:2694–2718. [PubMed: 28144341]
32. Genchev GZ, Kobayashi T, Lu H. Calcium induced regulation of skeletal troponin--computational insights from molecular dynamics simulations. PloS One. 2013; 8:e58313. [PubMed: 23554884]
33. Lindert S, Kekenes-Huskey PM, Huber G, Pierce L, McCammon JA. Dynamics and calcium association to the N-terminal regulatory domain of human cardiac troponin C: a multiscale computational study. The Journal of Physical Chemistry. B. 2012; 116:8449–8459. [PubMed: 22329450]
34. Sinko W, Lindert S, McCammon JA. Accounting for Receptor Flexibility and Enhanced Sampling Methods in Computer-Aided Drug Design. Chemical Biology & Drug Design. 2013; 81:41–49. [PubMed: 23253130]
35. Amaro RE, Baron R, McCammon JA. An improved relaxed complex scheme for receptor flexibility in computer-aided drug design. Journal of Computer-Aided Molecular Design. 2008; 22:693–705. [PubMed: 18196463]
36. Lin J-H, Perryman AL, Schames JR, McCammon JA. The relaxed complex method: Accommodating receptor flexibility for drug design with an improved scoring scheme. Biopolymers. 2003; 68:47–62. [PubMed: 12579579]

37. Lin J-H, Perryman AL, Schames JR, McCammon JA. Computational Drug Design Accommodating Receptor Flexibility:e The Relaxed Complex Scheme. Journal of the American Chemical Society. 2002; 124:5632–5633. [PubMed: 12010024]
38. Barakat K, Tuszynski J. Relaxed complex scheme suggests novel inhibitors for the lyase activity of DNA polymerase beta. Journal of Molecular Graphics and Modelling. 2011; 29:702–716. [PubMed: 21194999]
39. Barakat K, Mane J, Friesen D, Tuszynski J. Ensemble-based virtual screening reveals dual-inhibitors for the p53–MDM2/MDMX interactions. Journal of Molecular Graphics and Modelling. 2010; 28:555–568. [PubMed: 20056466]
40. Barakat KH, Torin Huzil J, Luchko T, Jordheim L, Dumontet C, Tuszynski J. Characterization of an inhibitory dynamic pharmacophore for the ERCC1–XPA interaction using a combined molecular dynamics and virtual screening approach. Journal of Molecular Graphics and Modelling. 2009; 28:113–130. [PubMed: 19473860]
41. Lindert S, Zhu W, Liu Y-L, Pang R, Oldfield E, McCammon JA. Farnesyl Diphosphate Synthase Inhibitors from In Silico Screening. Chemical Biology & Drug Design. 2013; 81:742–748. [PubMed: 23421555]
42. Lindert S, Tallorin L, Nguyen QG, Burkart MD, McCammon JA. In silico screening for Plasmodium falciparum enoyl-ACP reductase inhibitors. Journal of Computer-Aided Molecular Design. 2015; 29:79–87. [PubMed: 25344312]
43. Liu Y-L, Lindert S, Zhu W, Wang K, McCammon JA, Oldfield E. Taxodione and arenarone inhibit farnesyl diphosphate synthase by binding to the isopentenyl diphosphate site. Proceedings of the National Academy of Sciences. 2014; 111:E2530–E2539.
44. Menchon G, Bombarde O, Trivedi M, Négrel A, Inard C, Giudetti B, Baltas M, Milon A, Modesti M, Czaplicki G, Calsou P. Structure-Based Virtual Ligand Screening on the XRCC4/DNA Ligase IV Interface. Scientific Reports. 2016; 6:22878. [PubMed: 26964677]
45. Wong CF. Conformational transition paths harbor structures useful for aiding drug discovery and understanding enzymatic mechanisms in protein kinases. Protein Science: A Publication of the Protein Society. 2016; 25:192–203. [PubMed: 26032746]
46. Bhutani I, Loharch S, Gupta P, Madathil R, Parkesh R. Structure, dynamics, and interaction of Mycobacterium tuberculosis (Mtb) DprE1 and DprE2 examined by molecular modeling, simulation, and electrostatic studies. PloS One. 2015; 10:e0119771. [PubMed: 25789990]
47. Lindert S, Zhu W, Liu Y-L, Pang R, Oldfield E, McCammon JA. Farnesyl Diphosphate Synthase Inhibitors from In Silico Screening. Chemical Biology & Drug Design. 2013; 81:742–748. [PubMed: 23421555]
48. Geppert H, Vogt M, Bajorath J. Current Trends in Ligand-Based Virtual Screening: Molecular Representations, Data Mining Methods, New Application Areas, and Performance Evaluation. Journal of Chemical Information and Modeling. 2010; 50:205–216. [PubMed: 20088575]
49. Lyne PD. Structure-based virtual screening: an overview. Drug Discovery Today. 2002; 7:1047–1055. [PubMed: 12546894]
50. Wang X, Li MX, Sykes BD. Structure of the Regulatory N-domain of Human Cardiac Troponin C in Complex with Human Cardiac Troponin I147–163 and Bepridil. Journal of Biological Chemistry. 2002; 277:31124–31133. [PubMed: 12060657]
51. Li AY, Lee J, Borek D, Otwinowski Z, Tibbits GF, Paetzel M. Crystal Structure of Cardiac Troponin C Regulatory Domain in Complex with Cadmium and Deoxycholic Acid Reveals Novel Conformation. Journal of Molecular Biology. 2011; 413:699–711. [PubMed: 21920370]
52. Hoffman RMB, Sykes BD. Structure of the Inhibitor W7 Bound to the Regulatory Domain of Cardiac Troponin C. Biochemistry. 2009; 48:5541–5552. [PubMed: 19419198]
53. Durrant JD, de Oliveira CAF, McCammon JA. POVME: An Algorithm for Measuring Binding-Pocket Volumes. Journal of molecular graphics & modelling. 2011; 29:773–776. [PubMed: 21147010]
54. Sastry GM, Adzhigirey M, Day T, Annabhimoju R, Sherman W. Protein and ligand preparation: parameters, protocols, and influence on virtual screening enrichments. Journal of Computer-Aided Molecular Design. 2013; 27:221–234. [PubMed: 23579614]

55. Halgren TA, Murphy RB, Friesner RA, Beard HS, Frye LL, Pollard WT, Banks JL. Glide:e A New Approach for Rapid, Accurate Docking and Scoring. 2. Enrichment Factors in Database Screening. Journal of Medicinal Chemistry. 2004; 47:1750–1759. [PubMed: 15027866]
56. Friesner RA, Banks JL, Murphy RB, Halgren TA, Klicic JJ, Mainz DT, Repasky MP, Knoll EH, Shelley M, Perry JK, Shaw DE, Francis P, Shenkin PS. Glide:e A New Approach for Rapid, Accurate Docking and Scoring. 1. Method and Assessment of Docking Accuracy. Journal of Medicinal Chemistry. 2004; 47:1739–1749. [PubMed: 15027865]
57. Friesner RA, Murphy RB, Repasky MP, Frye LL, Greenwood JR, Halgren TA, Sanschagrin PC, Mainz DT. Extra Precision Glide:e Docking and Scoring Incorporating a Model of Hydrophobic Enclosure for Protein–Ligand Complexes. Journal of Medicinal Chemistry. 2006; 49:6177–6196. [PubMed: 17034125]
58. Banks JL, Beard HS, Cao Y, Cho AE, Damm W, Farid R, Felts AK, Halgren TA, Mainz DT, Maple JR, Murphy R, Philipp DM, Repasky MP, Zhang LY, Berne BJ, Friesner RA, Gallicchio E, Levy RM. Integrated Modeling Program, Applied Chemical Theory (IMPACT). Journal of Computational Chemistry. 2005; 26:1752–1780. [PubMed: 16211539]
59. *Maestro*, Schrodinger Release 2016–4. Schrodinger, LLC; New York, NY: 2016.
60. *LigPrep*, Schrodinger Release 2016–4. Schrodinger, LLC; New York, NY: 2016.
61. Greenwood JR, Calkins D, Sullivan AP, Shelley JC. Towards the comprehensive, rapid, and accurate prediction of the favorable tautomeric states of drug-like molecules in aqueous solution. Journal of Computer-Aided Molecular Design. 2010; 24:591–604. [PubMed: 20354892]
62. Shelley JC, Cholleti A, Frye LL, Greenwood JR, Timlin MR, Uchimaya M. Epik: a software program for pKa prediction and protonation state generation for drug-like molecules. Journal of Computer-Aided Molecular Design. 2007; 21:681–691. [PubMed: 17899391]
63. Harder E, Damm W, Maple J, Wu C, Reboul M, Xiang JY, Wang L, Lupyan D, Dahlgren MK, Knight JL, Kaus JW, Cerutti DS, Krilov G, Jorgensen WL, Abel R, Friesner RA. OPLS3: A Force Field Providing Broad Coverage of Drug-like Small Molecules and Proteins. Journal of Chemical Theory and Computation. 2016; 12:281–296. [PubMed: 26584231]
64. Shivakumar D, Williams J, Wu Y, Damm W, Shelley J, Sherman W. Prediction of Absolute Solvation Free Energies using Molecular Dynamics Free Energy Perturbation and the OPLS Force Field. Journal of Chemical Theory and Computation. 2010; 6:1509–1519. [PubMed: 26615687]
65. Jorgensen WL, Tirado-Rives J. The OPLS [optimized potentials for liquid simulations] potential functions for proteins, energy minimizations for crystals of cyclic peptides and crambin. Journal of the American Chemical Society. 1988; 110:1657–1666. [PubMed: 27557051]
66. Jorgensen WL, Maxwell DS, Tirado-Rives J. Development and Testing of the OPLS All-Atom Force Field on Conformational Energetics and Properties of Organic Liquids. Journal of the American Chemical Society. 1996; 118:11225–11236.
67. Triballeau N, Acher F, Brabet I, Pin J-P, Bertrand H-O. Virtual Screening Workflow Development Guided by the “Receiver Operating Characteristic” Curve Approach. Application to High-Throughput Docking on Metabotropic Glutamate Receptor Subtype 4. Journal of Medicinal Chemistry. 2005; 48:2534–2547. [PubMed: 15801843]
68. Hawkins PCD, Kelley BP, Warren GL. The Application of Statistical Methods to Cognate Docking: A Path Forward? Journal of Chemical Information and Modeling. 2014; 54:1339–1355. [PubMed: 24773409]
69. Davis JP, Norman C, Kobayashi T, Solaro RJ, Swartz DR, Tikunova SB. Effects of thin and thick filament proteins on calcium binding and exchange with cardiac troponin C. Biophysical Journal. 2007; 92:3195–3206. [PubMed: 17293397]
70. Siddiqui JK, Tikunova SB, Walton SD, Liu B, Meyer M, de Tombe PP, Neilson N, Kekenes-Huskey PM, Salhi HE, Janssen PML, Biesiadecki BJ, Davis JP. Myofilament Calcium Sensitivity: Consequences of the Effective Concentration of Troponin I. Frontiers in Physiology. 2016:7. [PubMed: 26903873]
71. Robertson S, Potter JD. The regulation of free Ca2+ ion concentration by metal chelators. Methods in Pharmacology. 1984; 5:63–75.
72. Feixas F, Lindert S, Sinko W, McCammon JA. Exploring the role of receptor flexibility in structure-based drug discovery. Biophysical Chemistry. 2014; 186:31–45. [PubMed: 24332165]

73. Sinko W, de Oliveira C, Williams S, Van Wynsberghe A, Durrant JD, Cao R, Oldfield E, McCammon JA. Applying Molecular Dynamics Simulations to Identify Rarely Sampled Ligand-bound Conformational States of Undecaprenyl Pyrophosphate Synthase, an Antibacterial Target. Chemical Biology & Drug Design. 2011; 77:412–420. [PubMed: 21294851]
74. Solaro RJ, Bousquet P, Johnson JD. Stimulation of cardiac myofilament force, ATPase activity and troponin C Ca++ binding by bepridil. Journal of Pharmacology and Experimental Therapeutics. 1986; 238:502–507. [PubMed: 2942677]
75. Williams, M., Malick, JB. Drug Discovery and Development. Springer Science & Business Media; Clifton, New Jersey: 2012. p. 453
76. Baell JB, Holloway GA. New Substructure Filters for Removal of Pan Assay Interference Compounds (PAINS) from Screening Libraries and for Their Exclusion in Bioassays. Journal of Medicinal Chemistry. 2010; 53:2719–2740. [PubMed: 20131845]
77. Dahlin JL, Nissink JWM, Strasser JM, Francis S, Higgins L, Zhou H, Zhang Z, Walters MA. PAINS in the Assay: Chemical Mechanisms of Assay Interference and Promiscuous Enzymatic Inhibition Observed during a Sulfhydryl-Scavenging HTS. Journal of Medicinal Chemistry. 2015; 58:2091–2113. [PubMed: 25634295]
78. Alland C, Moreews F, Boens D, Carpentier M, Chiusa S, Lonquety M, Renault N, Wong Y, Cantalloube H, Chomilier J, Hochez J, Pothier J, Villoutreix BO, Zagury JF, Tufféry P. RPBS: a web resource for structural bioinformatics. Nucleic Acids Research. 2005; 33:W44–W49. [PubMed: 15980507]
79. Néron B, Ménager H, Maufrais C, Joly N, Maupetit J, Letort S, Carrere S, Tuffery P, Letondal C. Mobyle: a new full web bioinformatics framework. Bioinformatics. 2009; 25:3005–3011. [PubMed: 19689959]
80. Lagorce D, Sperandio O, Baell JB, Miteva MA, Villoutreix BO. FAF-Drugs3: a web server for compound property calculation and chemical library design. Nucleic Acids Research. 2015; 43:W200–W207. [PubMed: 25883137]
81. Stepan AF, Walker DP, Bauman J, Price DA, Baillie TA, Kalgutkar AS, Aleo MD. Structural Alert/Reactive Metabolite Concept as Applied in Medicinal Chemistry to Mitigate the Risk of Idiosyncratic Drug Toxicity: A Perspective Based on the Critical Examination of Trends in the Top 200 Drugs Marketed in the United States. Chemical Research in Toxicology. 2011; 24:1345–1410. [PubMed: 21702456]
82. Abou-Gharbia M. Discovery of Innovative Small Molecule Therapeutics. Journal of Medicinal Chemistry. 2009; 52:2–9. [PubMed: 19072120]
83. Aldrich C, Bertozzi C, Georg GI, Kiessling L, Lindsley C, Liotta D, Merz KM, Schepartz A, Wang S. The Ecstasy and Agony of Assay Interference Compounds. ACS Central Science. 2017; 3:143–147. [PubMed: 28386587]
84. Vasquez-Martinez Y, Ohri RV, Kenyon V, Holman TR, Sepúlveda-Boza S. Structure–activity relationship studies of flavonoids as potent inhibitors of human platelet 12-hLO, reticulocyte 15-hLO-1, and prostate epithelial 15-hLO-2. Bioorganic & Medicinal Chemistry. 2007; 15:7408–7425. [PubMed: 17869117]
85. Cathcart MK, Folcik VA. Lipoxygenases and atherosclerosis: protection versus pathogenesis. Free Radical Biology and Medicine. 2000; 28:1726–1734. [PubMed: 10946214]
86. Neuzil J, Upston JM, Witting PK, Scott KF, Stocker R. Secretory Phospholipase A2 and Lipoprotein Lipase Enhance 15-Lipoxygenase-Induced Enzymic and Nonenzymic Lipid Peroxidation in Low-Density Lipoproteins†. Biochemistry. 1998; 37:9203–9210. [PubMed: 9636068]
87. Kayama Y, Minamino T, Toko H, Sakamoto M, Shimizu I, Takahashi H, Okada S, Tateno K, Moriya J, Yokoyama M, Nojima A, Yoshimura M, Egashira K, Aburatani H, Komuro I. Cardiac 12/15 lipoxygenase–induced inflammation is involved in heart failure. Journal of Experimental Medicine. 2009; 206:1565–1574. [PubMed: 19546247]
88. Backman TWH, Cao Y, Girke T. ChemMine tools: an online service for analyzing and clustering small molecules. Nucleic Acids Research. 2011; 39:W486–W491. [PubMed: 21576229]
89. Takeda S, Yamashita A, Maeda K, Maeda Y. Structure of the core domain of human cardiac troponin in the Ca2+-saturated form. Nature. 2003; 424:35–41. [PubMed: 12840750]

90. Ohio Supercomputer Center. Ohio Supercomputer Center. Columbus OH: Ohio Supercomputer Center; 1987. http://osc.edu/ark:/19495/f5s1ph73

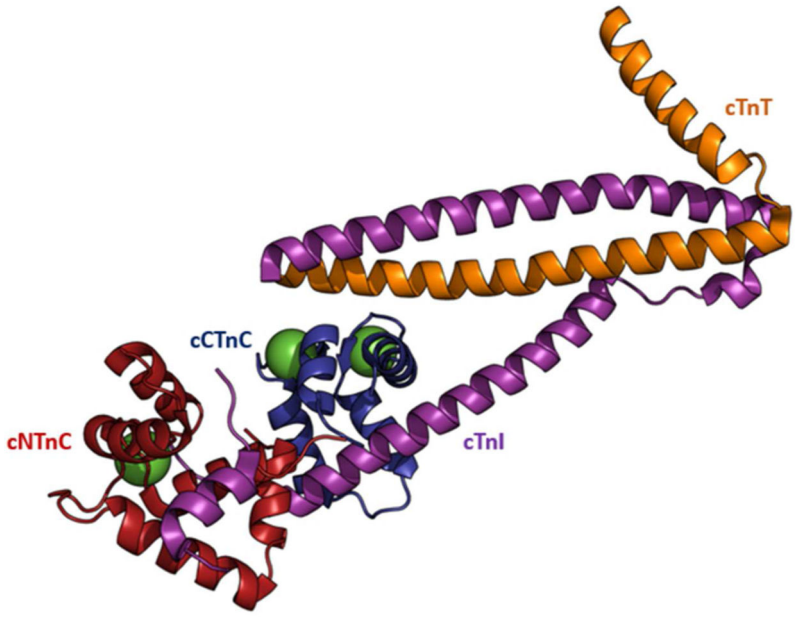


**Figure 1.**

Structure of cardiac troponin [PDB 1J1E[89]]. Each subunit is represented in a different color (cNTnC in red, cCTnC in blue, cTnI in purple, and cTnT in orange). The bound $Ca^{2+}$ ions are represented as green spheres.

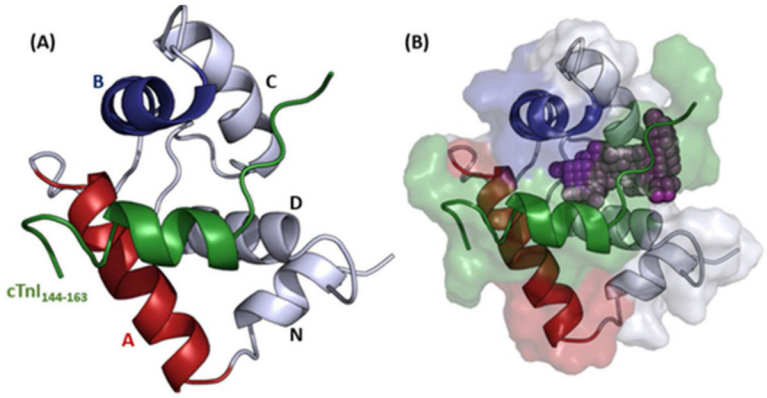


**Figure 2.**

N-terminal regulatory domain of troponin C (residues 1-89) complexed with the cTnI switch peptide (residues 144-163) [2L1R]. (A) shows the location of $cTnI_{144-163}$ between helices A and B of cNTnC. (B) shows the hydrophobic pocket between helices A and B represented as purple spheres.

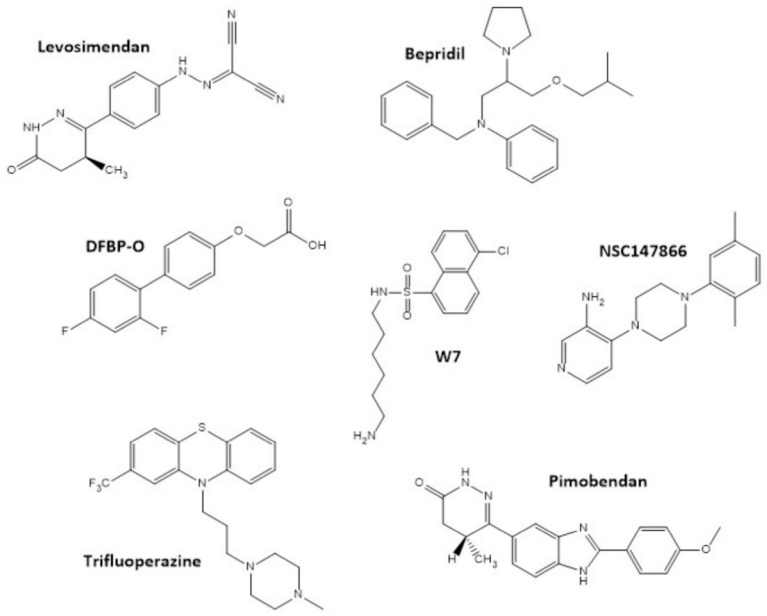


**Figure 3.**
Chemical structures of several calcium sensitizing compounds that bind to cNTnC.

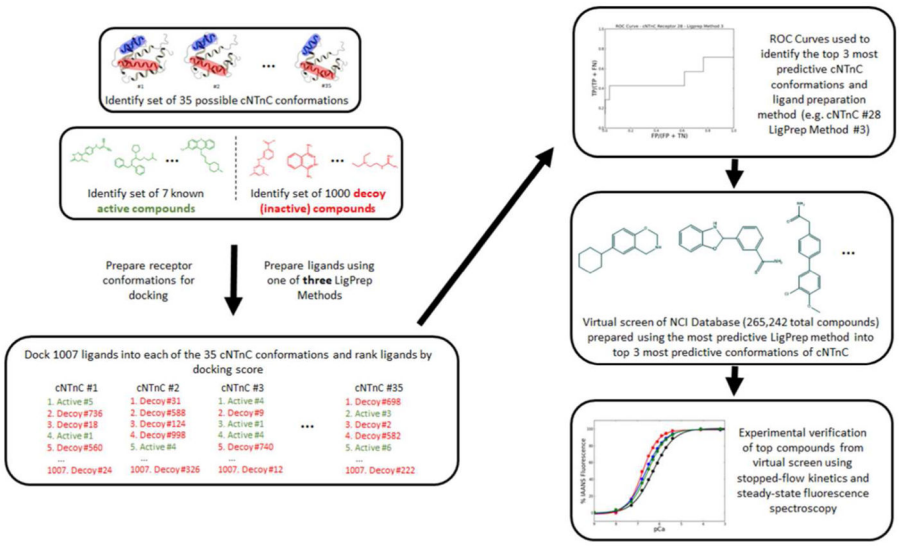


**Figure 4.**
Drug discovery protocol.

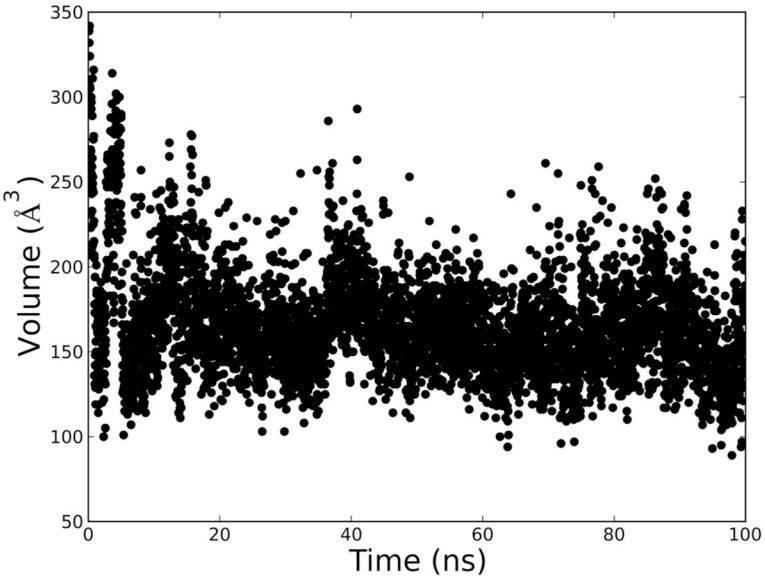


**Figure 5.**

Hydrophobic patch pocket-volumes calculated every 20 ps of a 100 ns MD trajectory of cNTnC F · $Ca^{2+}$-$cTnI_{144-163}$. Volumes, in units of $Å^3$, were calculated using POVME.

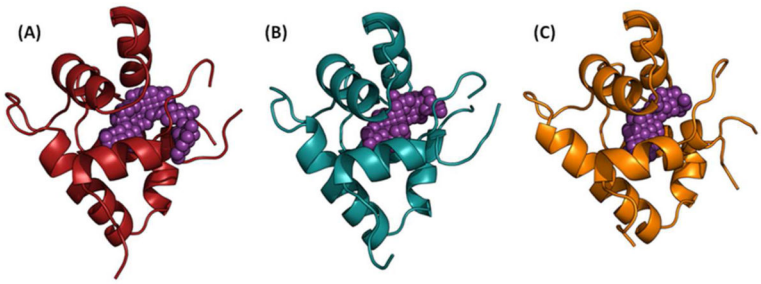


**Figure 6.**

Three cNTnC-cTnI$_{144\text{-}163}$ conformations identified as most predictive of ligand binding to the cNTnC hydrophobic pocket: (A) receptor #16, (B) receptor #19, and (C) receptor #28. The hydrophobic pockets are depicted by the purple spheres.

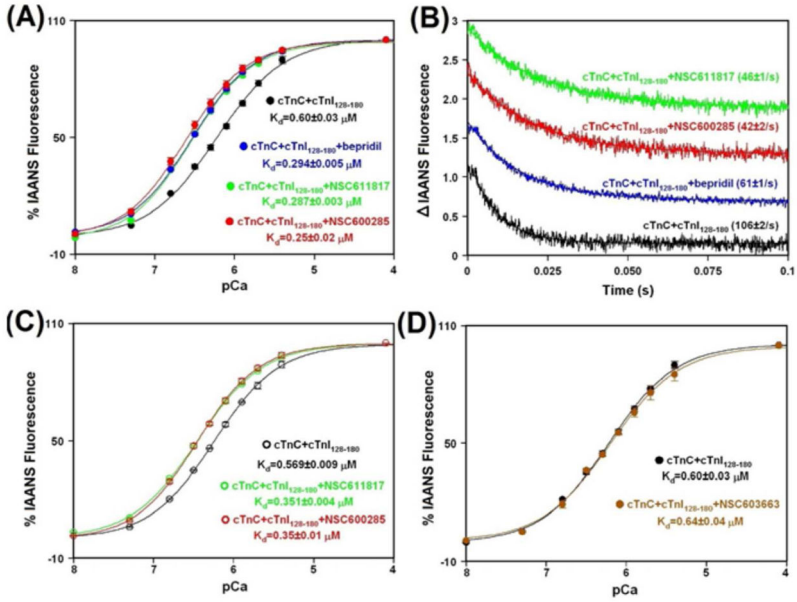


**Figure 7.**

The effect of NSC600285, NSC611817 and Bepridil on the $Ca^{2+}$ Binding Properties of cTnC in the Presence of $cTnI_{128\text{-}180}$. **Panel A** shows a plot of the steady-state $Ca^{2+}$ titrations performed in the absence or presence of compounds NSC600285, NSC611817 or bepridil, in the absence of the detergent Tween-80. This panel shows increases in IAANS fluorescence, which occur as $Ca^{2+}$ binds to IAANS-labeled $cTnC^{C35S}$ (0.25 μM), in the presence of $cTnI_{128\text{-}180}$ (1.25 μM), in the absence or presence of 100 μM of NSC600285, NSC611817 or bepridil at 15°C. The IAANS fluorescence was excited at 330 nm and monitored at 450 nm. **Panel B** shows the time course of decreases in IAANS fluorescence, measured in a stopped-flow apparatus, as $Ca^{2+}$ was removed by excess EGTA (10 mM), in the absence or presence of 100 μM of NSC600285, NSC611817 or bepridil, from IAANS-labeled $cTnC^{C35S}$ (0.5 μM), in the presence of $cTnI_{128\text{-}180}$ (2.5 μM), in the absence or presence of 100 μM of NSC600285, NSC611817 or bepridil at 15°C. Each trace is an average of at least five stopped-flow shots fit with a single exponential equation. The traces have been normalized and staggered for clarity. The IAANS fluorescence was excited at 330 nm and monitored through a 420-470 band-pass interference filter. **Panel C** depicts the results from experiments identical to those in Panel A but this time in the presence of the detergent Tween-80. This panel shows increases in IAANS fluorescence, which occur as $Ca^{2+}$ binds to IAANS-labeled $cTnC^{C35S}$ (0.25 μM), in the presence of $cTnI_{128\text{-}180}$ (1.25 μM), in the absence or presence of 100 μM of NSC600285 or NSC611817 at 15°C all in the presence of 0.025% Tween-80. **Panel D** shows a plot of the steady-state $Ca^{2+}$ titrations performed in the absence or presence of compound NSC603663, in the absence of the detergent Tween-80. This panel shows increases in IAANS fluorescence, which occur as $Ca^{2+}$ binds to IAANS-labeled $cTnC^{C35S}$ (0.25 μM), in the presence of $cTnI_{128\text{-}180}$ (1.25 μM), in the absence or presence of 100 μM of NSC603663 at 15°C.

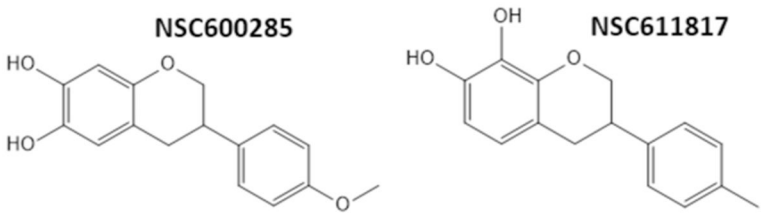


**Figure 8.**
Chemical structures of NSC600285 and NSC611817.

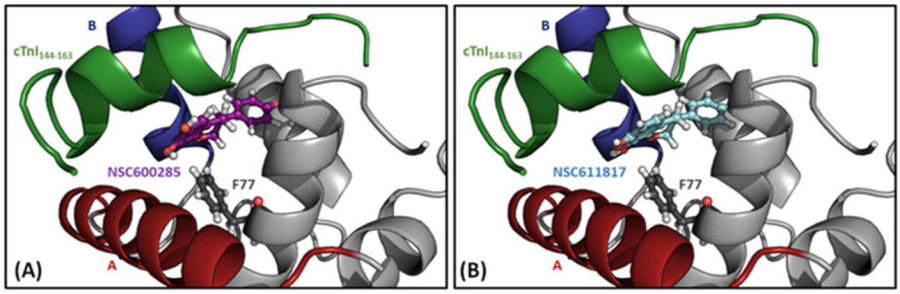


**Figure 9.**

Docked poses of NSC600285 (A) and NSC611817 (B) in conformation #28 of cNTnC-$cTnI_{144\text{-}163}$ with the residue F77 depicted.

**Table 1**

Table of three ligand preparation method parameters tested on the 1000 decoy and 7 active compounds.

| LigPrep Method | Ionization | Stereoisomers | Force Field | Generate Tautomers? | Generate at most per Ligand | Prepared Ligands Generated |
|---|---|---|---|---|---|---|
| 1 | - Generate possible states at target pH 7.4<br>- EPIK | Determine chiralities from 3D structures | OPLS_2005 | Yes | 5 | 1105 |
| 2 | - Generate possible states at target pH 7.4<br>- Ionizer | Determine chiralities from 3D structures | OPLS_2005 | Yes | 5 | 1392 |
| 3 | - Generate possible states at target pH 7.4<br>- Ionizer | Generate all combinations | OPLS_2005 | Yes | 5 | 1946 |

*J Chem Inf Model*. Author manuscript; available in PMC 2018 December 26.

**Table 2**

Results of the pocket-volume analysis of the receptor conformations selected from the 100 ns MD simulation of cNTnC · F $Ca^{2+}$-$cTnI_{144-163}$. Calculations were performed using POVME. RMSD calculations were performed over the entire cNTnC-$cTnI_{144-163}$ complex.

| Receptor | Volume (Å$^3$) | RMSD compared to 2L1R (Å) |
|---|---|---|
| 6 | 236 | 4.273 |
| 7 | 258 | 4.170 |
| 8 | 219 | 4.203 |
| 9 | 244 | 4.575 |
| 10 | 176 | 4.622 |
| 11 | 176 | 4.638 |
| 12 | 130 | 5.236 |
| 13 | 206 | 5.254 |
| 14 | 144 | 5.169 |
| 15 | 226 | 4.928 |
| 16 | 171 | 4.814 |
| 17 | 163 | 4.986 |
| 18 | 187 | 4.993 |
| 19 | 106 | 4.891 |
| 20 | 219 | 4.612 |

*J Chem Inf Model*. Author manuscript; available in PMC 2018 December 26.

**Table 3**

ROC curve results for LigPrep Methods 1, 2, and 3 and receptors #1–35. The reported areas under the curve and enrichment factors are relative to the baselines calculated for each ligand preparation method/receptor conformation pair. The receptors and the corresponding ligand preparation methods used for the virtual screening are bolded and italicized.

| | **LigPrep Method 1** | | **LigPrep Method 2** | | **LigPrep Method 3** | |
|---|---|---|---|---|---|---|
| **Receptor** | **Relative AUC** | **Relative EF** | **Relative AUC** | **Relative EF** | **Relative AUC** | **Relative EF** |
| 1 | −0.07 | −0.80 | 0.16 | −0.74 | 0.09 | −1.72 |
| 2 | −0.02 | −0.94 | −0.12 | −0.86 | −0.20 | −1.80 |
| 3 | 0.06 | 6.26 | 0.09 | −0.84 | 0.06 | 2.15 |
| 4 | 0.06 | −0.93 | 0.00 | −0.84 | −0.13 | 1.82 |
| 5 | −0.02 | −0.94 | −0.03 | −0.85 | −0.16 | −1.79 |
| 6 | 0.03 | −0.81 | 0.09 | −0.74 | 0.13 | −1.15 |
| 7 | 0.06 | 2.78 | 0.16 | −0.66 | 0.11 | −1.31 |
| 8 | 0.00 | 2.78 | 0.15 | 2.95 | −0.01 | 2.27 |
| 9 | 0.15 | 6.22 | 0.10 | −0.90 | −0.04 | 1.66 |
| 10 | 0.21 | 6.56 | 0.22 | 2.70 | 0.12 | 2.02 |
| 11 | 0.15 | −0.68 | 0.07 | −0.87 | 0.00 | 2.20 |
| 12 | 0.15 | −0.63 | 0.12 | −0.64 | 0.11 | 2.39 |
| 13 | 0.15 | 2.89 | 0.14 | 2.70 | 0.03 | 1.95 |
| 14 | 0.13 | 2.76 | 0.12 | 2.72 | 0.02 | 1.85 |
| 15 | −0.10 | 2.64 | −0.01 | −0.86 | −0.13 | −1.81 |
| ***16*** | 0.10 | −0.82 | 0.16 | −0.66 | ***0.12*** | ***2.42*** |
| 17 | 0.08 | −0.85 | 0.12 | −0.78 | −0.01 | −1.51 |
| 18 | 0.00 | −0.86 | 0.07 | −0.80 | −0.05 | −1.47 |
| ***19*** | 0.06 | 3.12 | 0.09 | 3.08 | ***0.08*** | ***2.56*** |
| 20 | 0.02 | −0.94 | 0.05 | −0.86 | −0.06 | −1.83 |
| 21 | −0.07 | −0.94 | −0.12 | −0.86 | −0.18 | −1.82 |
| 22 | 0.12 | −0.60 | 0.14 | −0.60 | 0.09 | −0.87 |
| 23 | 0.19 | −0.72 | 0.20 | −0.70 | 0.06 | −1.34 |
| 24 | −0.14 | −0.95 | −0.13 | −0.77 | −0.15 | −1.74 |

| | LigPrep Method 1 | | LigPrep Method 2 | | LigPrep Method 3 | |
|---|---|---|---|---|---|---|
| **Receptor** | **Relative AUC** | **Relative EF** | **Relative AUC** | **Relative EF** | **Relative AUC** | **Relative EF** |
| 25 | −0.15 | −0.95 | −0.07 | −0.85 | −0.08 | −1.81 |
| 26 | 0.00 | −0.97 | 0.02 | −0.87 | −0.04 | −1.78 |
| 27 | −0.05 | −0.94 | −0.07 | −0.85 | −0.07 | 1.80 |
| ***28*** | 0.04 | −0.82 | 0.10 | 6.40 | ***0.04*** | ***9.55*** |
| 29 | 0.15 | −0.75 | 0.18 | −0.74 | 0.11 | 2.27 |
| 30 | −0.07 | −0.55 | −0.04 | −0.54 | −0.01 | −1.18 |
| 31 | −0.06 | −0.44 | 0.04 | −0.23 | 0.00 | −0.58 |
| 32 | 0.10 | 2.87 | 0.11 | −0.70 | 0.02 | −1.26 |
| 33 | 0.04 | −0.94 | 0.12 | 2.75 | −0.03 | 1.94 |
| 34 | −0.05 | −0.95 | −0.01 | −0.86 | −0.01 | −1.81 |
| 35 | −0.02 | −0.94 | 0.01 | 2.75 | −0.08 | 1.79 |
| **Total Positive** | 22 | 10 | 25 | 8 | 17 | 16 |

**Table 4**

Top results from virtual drug screenings of the NCI Database and both subsets of the NCI Database. The initial screen comprised of the entire NCI Database and the subset of compounds similar to NSC147866. Shown are the NSC identification numbers of each compound along with their average docking score over the three receptors as well as their molecular weight.

| Initial Screen of Compounds | | | Screen of Compounds Similar to NSC600285 | | |
|---|---|---|---|---|---|
| **NSC** | **Avg. Docking Score** | **Molecular Weight (g/mol)** | **NSC** | **Avg. Docking Score** | **Molecular Weight (g/mol)** |
| 254212 | −10.09 | 339.27 | 611817 | −10.21 | 256.30 |
| 600285 | −7.69 | 272.30 | 611815 | −10.16 | 258.27 |
| 600286 | −7.58 | 256.30 | 611816 | −10.05 | 272.30 |
| 24047 | −6.79 | 300.40 | 603663 | −9.77 | 302.33 |
| 24045 | −6.73 | 286.38 | 93367 | −9.19 | 272.30 |
| 67598 | −6.45 | 248.33 | 26182 | −8.21 | 412.48 |
| 202117 | −6.42 | 285.41 | 600291 | −6.08 | 300.35 |
| 170630 | −6.25 | 270.33 | 157109 | −5.78 | 390.48 |
| 77134 | −6.14 | 259.35 | 605546 | −5.65 | 368.39 |
| 671841 | −5.98 | 232.71 | 628872 | −4.03 | 344.36 |
| 34046 | −5.95 | 252.36 | 27593 | −3.68 | 410.47 |
| 269897 | −5.76 | 224.30 | 102052 | −2.70 | 328.36 |
| 19841 | −5.56 | 198.27 | 681610 | −2.66 | 284.31 |
| 147896 | −5.07 | 304.39 | 27594 | −2.55 | 438.52 |
| | | | 55274 | −2.54 | 330.34 |
| | | | 16317 | −1.77 | 240.30 |